

# Optical spectral analysis of the nonlinear dynamics in long-wavelength single-mode VCSELs subject to orthogonal optical injection

A. Quirce<sup>1,2</sup>, P. Pérez<sup>1,2</sup>, A. Valle<sup>1\*</sup>, and L. Pesquera<sup>1</sup>.

<sup>1</sup>Instituto de Física de Cantabria, CSIC-Universidad de Cantabria, Avda. Los Castros s/n, E-39005, Santander, Spain.

<sup>2</sup>Departamento de Física Moderna, Universidad de Cantabria, Avda. Los Castros s/n, E-39005, Santander, Spain

## ABSTRACT

We report an experimental study of the polarization-resolved nonlinear dynamics of a 1550nm single-mode linearly polarized VCSEL when subject to orthogonal optical injection. We measure high-resolution (10 MHz) optical spectra of the linear polarizations and the total power emitted by the VCSEL. Spectra are analyzed together with the simultaneous temporal series of linearly polarized powers. For periodic dynamics, both linear polarizations show spectra with equally spaced peaks with a separation that corresponds to the frequency detuning. As the injected power increases much more peaks are observed with larger (smaller) separation between them when the frequency detuning is positive (negative). For negative values of the frequency detuning, increasing the injected power leads to irregular dynamics that is characterized by optical spectra for both linear polarizations with broad pedestals and much less defined peaks specially for the parallel polarization.

**Keywords:** Semiconductor lasers, vertical-cavity surface-emitting laser (VCSEL), polarization switching, injection locking, nonlinear dynamics.

## INTRODUCTION

Semiconductor lasers exhibit a rich variety of nonlinear dynamical behaviors [1]. These are usually induced by applying optical or opto-electronic feedback, modulation of the injected current or an external optical injection [1]. There has been a lot of interest in the nonlinear dynamics of a special type of semiconductor lasers, the vertical-cavity surface-emitting lasers (VCSELs), because of their special characteristics. These include single-longitudinal mode operation, circular beam profile, reduced fabrication costs, ease of fabrication of 2D arrays, etc. [2]. These devices offer additional degrees of freedom, like the direction of the emitted polarization and the presence of multiple transverse modes, when compared with their edge-emitting counterparts. A variety of phenomena related to their polarization and transverse mode characteristics appear in these devices. For instance, the direction of the polarization can change when changing the bias current [3-4], mode locking between transverse modes can occur [5], or turn-off-induced pulsations can appear when modulating the bias current [6-7].

The performance of VCSELs can be improved by injecting light emitted by another laser. The optical injection technique can be used for reducing the laser linewidth, the mode partition noise or for enhancing the modulation bandwidth without modifying the semiconductor laser design [8-11]. Optical injection in VCSELs is also interesting from the fundamental point of view because a wealth of complex nonlinear dynamics and bifurcations are obtained. These include period doubling, quasiperiodicity, chaos, injection locking, polarization switching (PS) and optical bistability [12-34]. Early experiments considered devices in which the polarizations of both the VCSEL and the optical injection were parallel [12-13].

\*e-mail: [valle@ifca.unican.es](mailto:valle@ifca.unican.es); phone 34 942 201465; fax: 34 942 200935

However, most of the studies have been performed using the so called “orthogonal optical injection” [14-34]. In this configuration linearly polarized light from an external laser is injected orthogonally to the linear polarization of a free-running VCSEL [14]. A lot of attention has been paid recently to the effects of orthogonal optical injection on long-wavelength devices because of their applications in present and future optical telecommunication networks [26-34]. These studies have been performed using devices characterized by large values of the birefringence parameter and by emission in a single linear polarization over the whole bias current range in absence of optical injection.

Nonlinear dynamics of these systems has been analyzed by using stability maps. These maps have been obtained using the RF spectra of the total power to identify the boundaries between regions of different behavior [31-34]. Periodic dynamics, PS and irregular and possibly chaotic behaviour were obtained [34]. The analysis of the dynamics has been complemented with measurements of simultaneous time traces and RF spectra of both linearly polarized output signals [32-34]. Optical spectra of the total and polarized emissions have also been obtained in order to characterize the dynamics [32]. These spectra were obtained with a Fabry-Perot analyzer with a resolution of 4 pm. Optical spectra with better resolution are desirable in order to have a better description of the dynamics of the system.

In this work we extend the experimental study of [32,34] by measuring high-resolution polarization-resolved optical spectra of a long-wavelength VCSEL when subject to orthogonal optical injection. A high resolution optical spectrum analyzer (BOSA) with very high optical resolution (0.08 pm  $\sim$ 10 MHz) was used in our measurements. Our VCSEL is the same device studied in [32,34]. In this way we measure the optical spectra that characterize the simultaneous time traces and RF spectra obtained in [32,34]. Attention is paid to the dependence of the dynamics on the injected power, on the detuning between the frequency of the injected signal and the free-running frequency of the orthogonal polarization of the VCSEL, and on the bias current applied to the device.

Our paper is organized as follows. The experimental results for the nonlinear dynamics for small and large values of the bias current are analyzed in sections II and III, respectively. Finally, in section IV, a summary and conclusions are presented.

## II. EXPERIMENTAL RESULTS: SMALL BIAS CURRENT

We have used an all-fibre set-up in order to inject light from a tunable laser into a quantum-well 1550 nm VCSEL. The set-up is similar to that used in [32,34]. The same commercially available VCSEL (Raycan) has been used in our experiments. The VCSEL bias current and temperature are controlled, respectively, by a laser driver and a temperature controller. The temperature is held constant at 298 °K during the experiments.

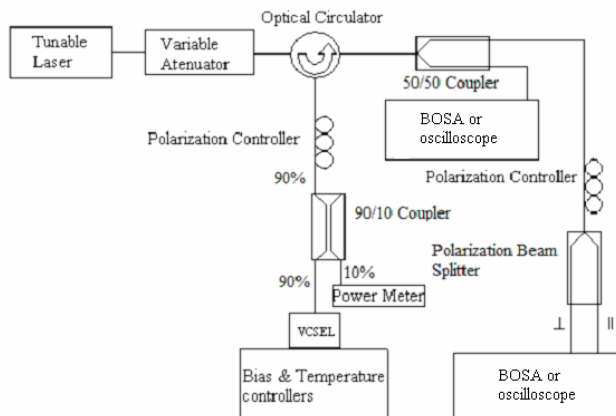


Fig. 1. Experimental set-up of orthogonal optical injection in a VCSEL.

A variable optical attenuator is included after the tunable laser to control the power of the optical injection. The output of the tunable laser is then injected into the VCSEL using a three-port optical circulator. Orthogonal optical injection is

obtained by using a fibre polarization controller connected to the second port of the circulator. A 90/10 fibre directional coupler divides the optical path in two branches; the 10% branch is used to monitor the optical input power with a power meter whereas the 90% output is directly connected to the VCSEL. The reflected output of the VCSEL is analyzed by connecting different measurement equipment to the third port of the circulator. One half of the power is used to obtain the time traces of the total power at the oscilloscope with bandwidth of 6 GHz. The oscilloscope is substituted by a high-resolution optical spectrum analyzer (BOSA) for measuring the optical spectra. The other half of the power is directed to a polarization beam splitter that selects the polarization direction in which the time traces of the power are measured. Two similar high speed photodetectors (9 GHz bandwidth) were connected before the oscilloscope for measuring simultaneously the time traces.

The L-I curve of the free-running VCSEL is shown in [32, Fig. 2a]. The VCSEL emits in the fundamental transverse mode with a threshold current of  $I_{th}=1.64$  mA. The VCSEL emits in a linear polarization which we will call the “parallel” polarization. Emission in the parallel polarized fundamental mode is obtained along the whole current range. Fig. 2(b) of [32] shows the low-resolution optical spectrum of the VCSEL biased at 8 mA. The lasing mode of the device with parallel polarization is located at the wavelength  $\lambda_{||} = 1536.6$  nm. The subsidiary mode corresponds to the fundamental transverse mode with “orthogonal” polarization and its wavelength ( $\lambda_{\perp}$ ) is shifted 0.49 nm to the long-wavelength side of the lasing mode. This value for the frequency splitting between the two orthogonal polarizations is very large in comparison to those reported in short-wavelength devices [23]. Spectra of this form are measured for all biases and no PS is observed for bias current above the threshold value.

The dynamical behavior of our system has been summarized by using stability maps [32,34] for different values of the bias current applied to the VCSEL. In these maps RF spectra of the total power are used to distinguish between different dynamical regimes. The optical injection is characterized by its strength, given by the value of the optical power arriving at the VCSEL,  $P_{inj}$ , and by its frequency,  $\nu_{inj}$ . We consider values of  $\nu_{inj}$ , that are close to the frequency of the perpendicular polarization,  $\nu_{\perp}$ , the frequency detuning being  $\Delta\nu = \nu_{inj} - \nu_{\perp}$ . In these stability maps different dynamical behaviors are plotted with different colours in the  $\Delta\nu - P_{inj}$  plane. The stability map of Fig. 2 of [34] shows that periodic (period 1 and period doubling) behaviour, irregular and possibly chaotic dynamics, and stable locking regions appear in this system.

In this section experimental results corresponding to a small value of the bias current,  $I=4$ mA, are presented. We show in the left column of Fig. 2 the results relative to simultaneous measurements of linearly polarized temporal traces. Results of Fig. 2 correspond to a fixed frequency detuning of  $\Delta\nu=4$  GHz and different values of  $P_{inj}$ . These values are the same than those considered in [34]. Corresponding optical spectra for the total power are shown in the right column of Fig. 2. Showing results for the total power is enough to describe the optical spectra of both linear polarizations. We have checked that optical spectra of the orthogonal (parallel) polarization correspond to the optical spectra of the total emitted light below (above) 0 GHz. The zero value of the frequency has been chosen to correspond to  $\nu_{th} = (\nu_{\perp} + \nu_{||})/2$ , that is the intermediate value between the frequencies of both linear polarizations. Fig.2(a) shows that oscillations of small amplitude around the steady state characterize both linear polarizations and the total power. This behavior corresponds to a point near the period 1 (P1) region in the stability map [34]. Several peaks appear in the optical spectrum: the first one, at -31 GHz, corresponds to the orthogonal polarization, the second one, at 4.4 GHz to the right, corresponds to the optical injection, and the last one, at 31.5 GHz corresponds to the parallel polarization. RF spectra shows also a peak at 4.4 GHz [34]. A clear P1 dynamics in the total and orthogonal polarized powers is obtained when increasing  $P_{inj}$  as it is shown in Fig. 2 (c). Fig. 2(d) shows that the optical spectrum of the orthogonal and parallel polarizations have more peaks than in Fig. 2(b). They are equally spaced around a value of 4.6 GHz. This value also corresponds to the frequency at which the RF spectra of the orthogonal and total power have a well defined peak [34]. The separation between consecutive peaks in the optical spectrum increases as  $P_{inj}$  increases. This can be explained in terms of the “frequency pushing” effect [34]. P1 dynamics is caused by beating between the optical injection and the orthogonal mode of the VCSEL. Further increase of  $P_{inj}$  produces PS: the peak corresponding to the parallel polarization is no longer observed in Fig. 2(f). Fig. 2(e) shows that the orthogonal polarization power is oscillating at a frequency around 5.3 GHz. The amplitude of the oscillations decrease when increasing  $P_{inj}$  as it is shown in Fig. 2(g). Operation in the stable locking (SL) regime is illustrated in the lower part of Fig. 2. The amplitude of the oscillations in the time traces is very small (see Fig. 2(i)) and the orthogonal polarization mode is stably locked to the optical injection (see Fig. 2(j)). Flat RF spectra, characteristic of SL regime, are also observed [34].

Fig. 3 shows the time traces and optical spectra for a negative value of the frequency detuning,  $\Delta\nu=-2$  GHz. Figs. 3(a-b) illustrate the behavior obtained for small values of  $P_{inj}$ , in such a way that the system is in the P1 regime. Non-sinusoidal periodic dynamics are obtained for both periodic dynamics, in contrast with the positive  $\Delta\nu$  case.

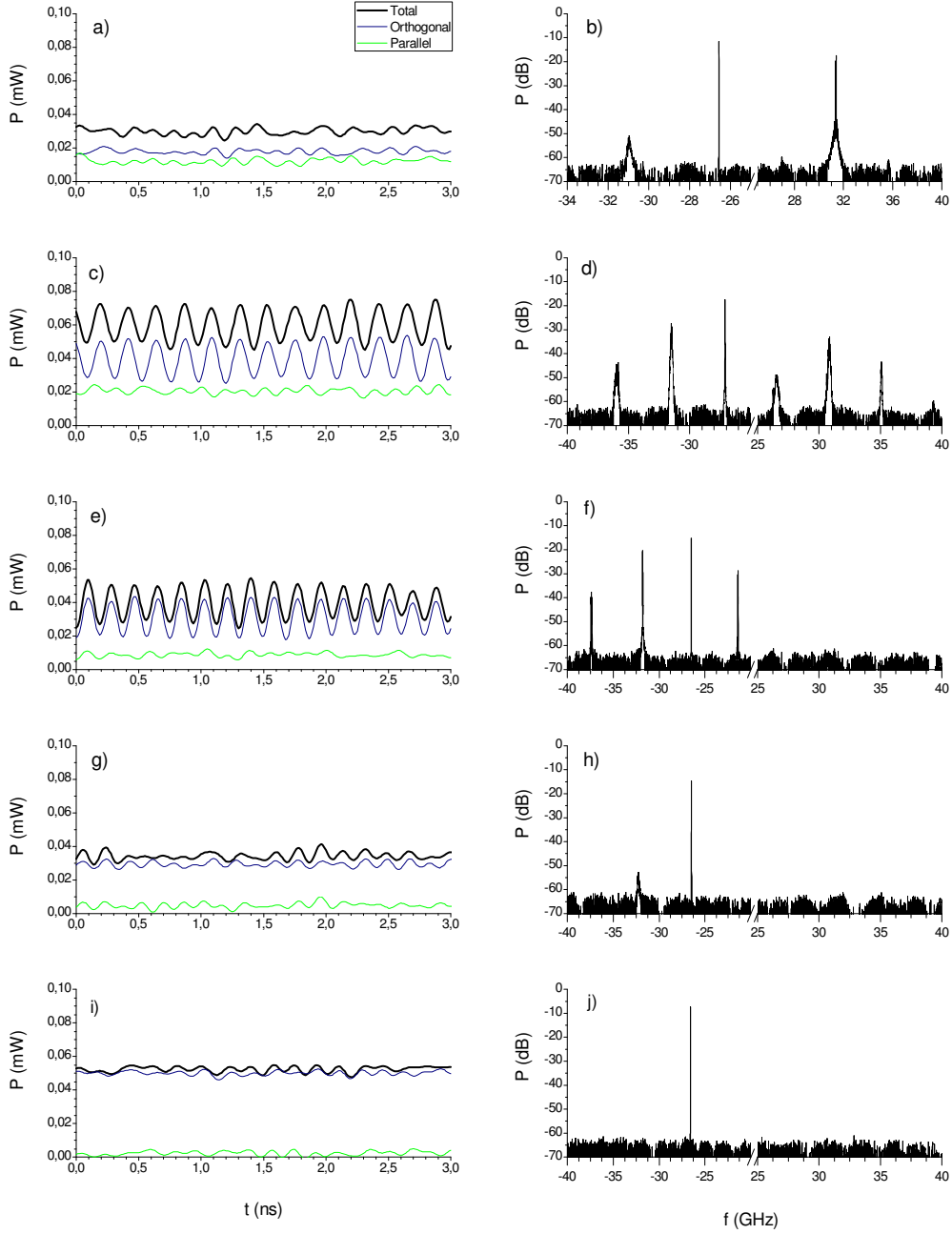


Fig. 2. (Left column) Time traces of the total power and of the power of both linear polarizations. (Right column) Optical spectra of the total power. Several values of injected power are considered: (a,b)  $P_{inj} = 47 \mu\text{W}$ , (c,d)  $P_{inj} = 76.4 \mu\text{W}$ , (e,f)  $P_{inj} = 158 \mu\text{W}$ , (g,h)  $P_{inj} = 240.3 \mu\text{W}$ , and (i,j)  $P_{inj} = 1275.5 \mu\text{W}$ . The frequency detuning is  $\Delta\nu = 4 \text{ GHz}$  and the bias current is 4 mA.

The optical spectrum of the orthogonal and parallel polarizations have multiple peaks. The separation between consecutive peaks is around 1.9 GHz, that is the value at which the RF spectra have their fundamental frequency [34].

Fig. 3 (c) shows that the power of the parallel polarization consists of a train of large amplitude pulses that are responsible for the large amplitude pulses of the total power. The shoulder that appears in the total power after those pulses is due to the contribution of the orthogonally polarized mode.

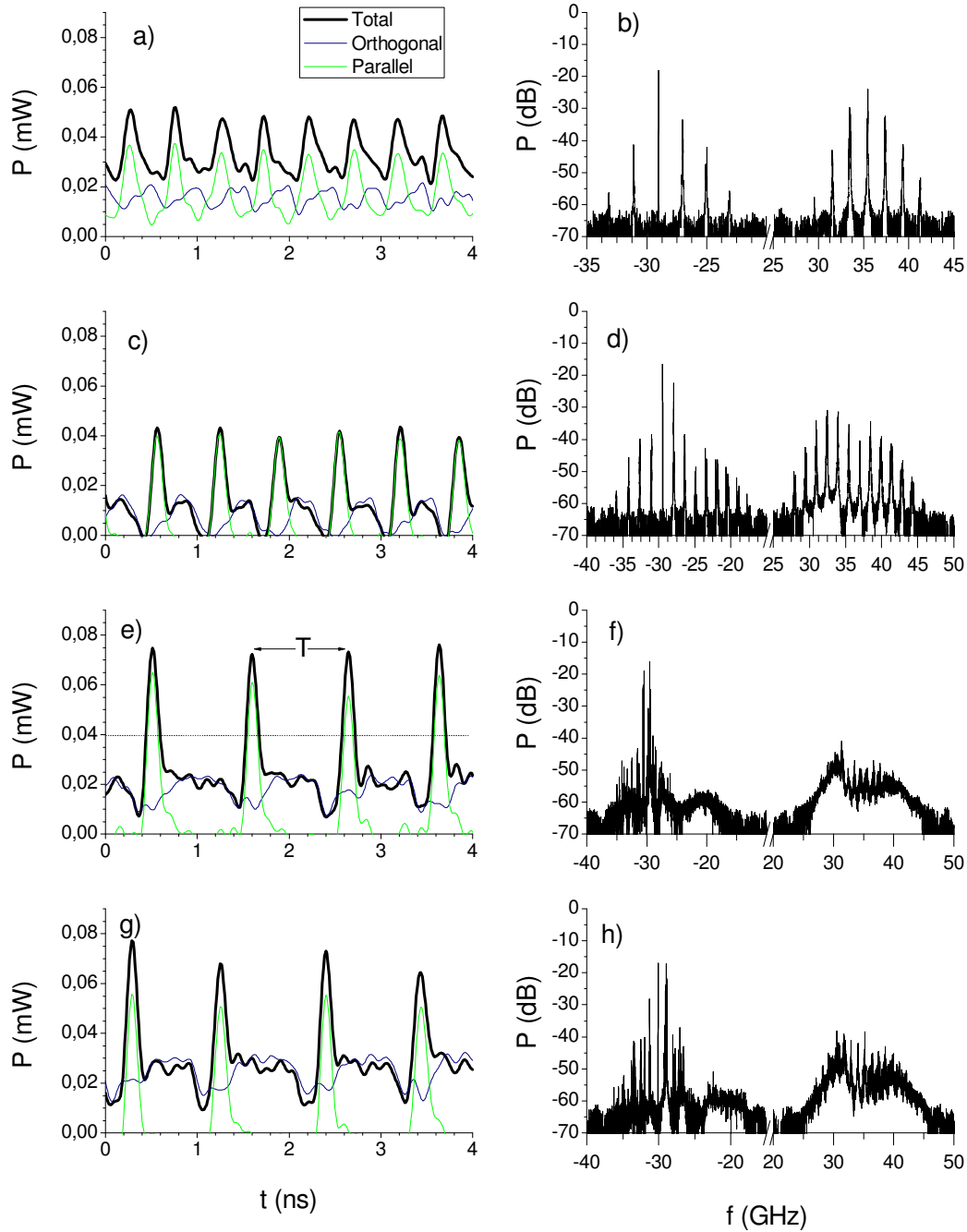


Fig. 3. (Left column) Time traces of the total power and of the power of both linear polarizations. (Right column) Optical spectra of the total power. Several values of injected power are considered: (a,b)  $P_{inj} = 26.9 \mu\text{W}$ , (c,d)  $P_{inj} = 35.5 \mu\text{W}$ , (e,f)  $P_{inj} = 42.4 \mu\text{W}$ , and (g,h)  $P_{inj} = 53.6 \mu\text{W}$ . The frequency detuning is  $\Delta\nu = -2 \text{ GHz}$  and the applied bias current is 4 mA.

Comparison between Fig. 3(b) and Fig. 3 (d) shows that the number of peaks in the optical spectra of both linear polarizations increases as  $P_{inj}$  is increased. Also the separation between consecutive peaks decreases to 1.5 GHz in Fig. 3(d). This can be explained in terms of a “frequency pulling” effect [34]. This frequency also corresponds to the value at which the RF spectra have their fundamental frequency [34]. Figs. 3(e)-(h) illustrate the irregular dynamical behavior that is obtained when increasing  $P_{inj}$ . This dynamics is characterized by broad RF spectra in which the peaks tend to disappear (see Fig. 4(e), and 4(g) of [34]). Fig. 3(f) and Fig. 3(h) show the corresponding optical spectra. Irregular dynamics is characterized by optical spectra for both linear polarizations with wide pedestals and much less defined peaks with smaller separation between them.

Temporal dynamics can be characterized also by the interpulse time,  $T$ , illustrated in Fig. 3(e). This time is defined as the time between consecutive pulses, larger than a chosen reference level. The level used in this figure is also plotted in Fig. 3(e) with a dotted line. Broadening of the optical and RF spectra is related to a large increase of the interpulse time dispersion,  $\sigma_T$ . This is illustrated in Table 1 in which the average value of  $T$ ,  $\langle T \rangle$ , and  $\sigma_T$  are shown for different values of  $P_{inj}$ .

$\Delta\nu/\text{GHz}$	$P_{inj}/\mu\text{W}$	$\langle T \rangle/\text{ns}$	$\sigma_T/\text{ps}$	$C(0)$	$C(\tau_m)$	$\tau_m/\text{ns}$
4	47.0	0.22	60	0.006	0.006	0
	76.4	0.22	8	-0.12	-0.21	0.0375
	158.0	0.19	6	0.014	0.036	-0.0375
	240.3	0.18	40	0.002	0.019	-0.05
-2	26.9	0.52	17	-0.54	-0.85	0.075
	35.5	0.66	12	-0.51	-0.76	0.1
	42.4	0.93	40	-0.48	-0.64	0.175
	53.6	1.04	96	-0.50	-0.66	0.187

Table 1: Averaged interpulse time ( $\langle T \rangle$ ), standard deviation ( $\sigma_T$ ), and correlation coefficient ( $C(0)$ ), first minimum of the cross-correlation function ( $C(\tau_m)$ ) and time at which it appears ( $\tau_m$ ). The applied bias current is 4 mA

The correlation properties between the power of the parallel,  $P_{\parallel}(t)$ , and the orthogonal,  $P_{\perp}(t)$ , linear polarizations can be discussed in terms of their cross correlation function,  $C(\tau)$  given by

$$C(\tau) = \frac{\overline{(P_{\parallel}(t+\tau) - \overline{P_{\parallel}})(P_{\perp}(t) - \overline{P_{\perp}})}}{\sigma_{\parallel}\sigma_{\perp}}$$

where the bar means time averaging operation and  $\sigma_i^2 = \overline{(P_i(t) - \overline{P_i})^2}$ ,  $i=\parallel, \perp$ . Temporal averages have been performed by using time series of 500 ns duration. When  $\Delta\nu < 0$  anticorrelated behavior between the power of both linear polarizations is clear from the time traces shown in Fig. 3 and from the values of  $C(0)$  shown in Table 1. However, when  $\Delta\nu > 0$  the correlation between both linear polarizations is very weak as seen from Fig.2 and Table 2.

### III. EXPERIMENTAL RESULTS: LARGE BIAS CURRENT

In this section we present experimental results corresponding to a large value of the bias current,  $I=8\text{mA}$ . We show in Fig. 4 the results corresponding to a fixed frequency detuning of  $\Delta\nu=5$  GHz and different values of  $P_{inj}$ .  $\Delta\nu$  and  $P_{inj}$  values are similar to those considered in [34]. In Fig. 4(a) sinusoidal time traces are found for the power of both linear polarizations. These time traces have a correlated behavior as it can also be seen in Table 2. The optical spectrum of each linear polarization consists in several peaks as it can be seen in Fig. 4(b). The peak that corresponds to the optical injection is the one appearing near the -25 GHz frequency. Consecutive peaks are separated by an averaged value of 5.4 GHz. This value is very similar to the value at which RF spectra have a well defined peak (5.5 GHz) [34]. P1 dynamics is more clear when increasing  $P_{inj}$  as it can be seen in Fig. 4(c) because the total power has more regular oscillations with

larger amplitudes. Fig. 4(d) and Fig. 4(f) show that the number of peaks in the optical spectrum of the orthogonal polarization is larger as  $P_{inj}$  is increased. The separation between consecutive peaks in Fig. 4(f) is around 6.2 GHz. The magnitude of the peaks in the spectrum of the parallel polarization decreases because the PS region is approached. Figs. 4(e-f) show that only the orthogonal polarization contributes to the dynamics of the total power. RF spectra corresponding to Figs. 4(e-h) show weak period doubling dynamics [34] that we were not able to appreciate in the optical spectrum. Fig. 4(h) shows that PS has been achieved when  $P_{inj}=287.8\ \mu\text{W}$ . Further increase of  $P_{inj}$  leads to SL dynamics, as it is shown in Figs. 4(i-j).

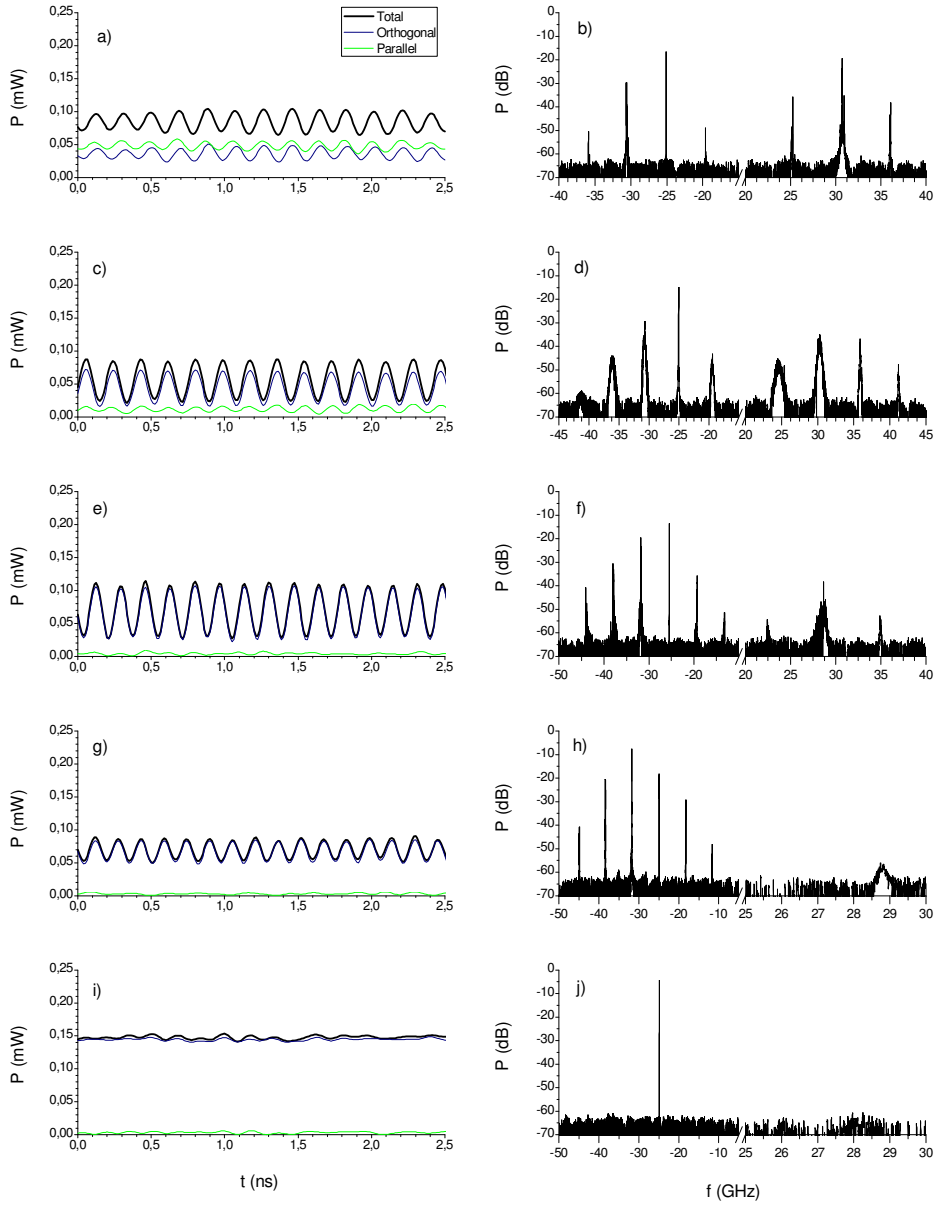


Fig. 4. (Left column) Time traces of the total power and of the power of both linear polarizations. (Right column) Optical spectra of the total power. Several values of injected power are considered: (a,b)  $P_{inj}=96.1\ \mu\text{W}$ , (c,d)  $P_{inj}=127.6\ \mu\text{W}$ , (e,f)  $P_{inj}=197.3\ \mu\text{W}$ , (g,h)  $P_{inj}=287.8\ \mu\text{W}$ , and (i,j)  $P_{inj}=3301.8\ \mu\text{W}$ . The frequency detuning is  $\Delta\nu=5\ \text{GHz}$  and the applied bias current is 8 mA.

We now analyze the dynamics obtained for a negative  $\Delta\nu$  value. Fig.5 shows time traces and optical spectra when  $\Delta\nu = -1.5$  GHz. Figures 5(a) and 5(b) show the P1 dynamics that is obtained for low values of  $P_{inj}$ . The qualitative behaviour of the time traces is similar to that shown in Fig. 3(a). Maxima of the total power are due to the maxima of the power of the parallel polarization. Fig. 5(b) shows that there are several peaks in the optical spectra of the parallel and orthogonal polarization. They are separated by 3.3 GHz, a value that is similar to that found for the frequency of the fundamental peak (3 GHz) in the RF spectrum [34].

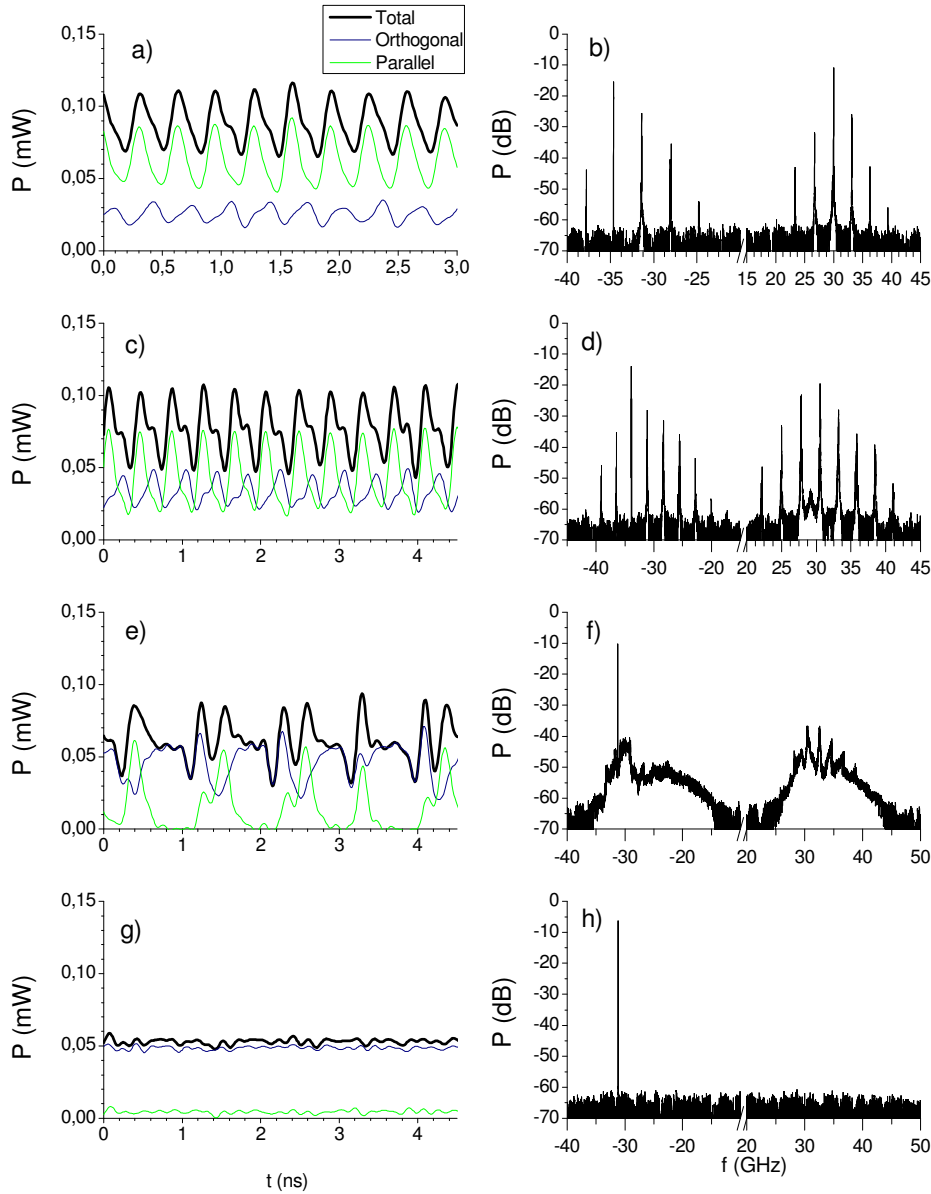


Fig. 5. (Left column) Time traces of the total power and of the power of both linear polarizations. (Right column) Optical spectra of the total power. Several values of injected power are considered: (a,b)  $P_{inj} = 58.5 \mu\text{W}$ , (c,d)  $P_{inj} = 67.6 \mu\text{W}$ , (e,f)  $P_{inj} = 84 \mu\text{W}$ , and (g,h)  $P_{inj} = 111.2 \mu\text{W}$ . The frequency detuning is  $\Delta\nu = -1.5$  GHz and the applied bias current is 8 mA.

Comparison between Fig. 5(b) and Fig. 5(d) shows that the number of peaks in the optical spectra of both linear polarizations increases as  $P_{inj}$  is increased. This behavior is similar to that found in Fig. 3(b) and 3(d). However, the approach to the SL dynamics as  $P_{inj}$  is increased is different to that found for small bias currents. First, weak period doubling dynamics is found for both linear polarizations and for the total power as it has been shown with the corresponding RF spectra [34]. The optical spectrum corresponding to this case is shown in Fig. 5(d). P2 dynamics is barely visible from the peak appearing near 29 GHz frequency. Second, further increase of  $P_{inj}$  leads to irregular behavior in both linear polarizations that is qualitatively different to that shown in Figs. 3(g-h). Time traces of Fig. 5(e) are much more irregular than those of Fig. 3(g) because two large amplitude consecutive pulses are occasionally fired in the total power. Also RF spectra corresponding to Fig. 5(e) are much broader than those corresponding to Fig. 3(g) [34]. The corresponding optical spectra are shown in Fig. 5(f). The optical spectrum corresponding to the orthogonal polarization consists in a very intense peak at the frequency of the optical injection and a very wide pedestal characterized by two maxima that appear near -30 and -24 GHz. The parallel polarization is also characterized by a wide optical spectrum with some peaks still visible between 30 and 35 GHz. Increasing  $P_{inj}$  leads to a simultaneous appearance of PS and SL, as it is illustrated in Figs. 5(g-h): only the optical spectrum corresponding to the orthogonal polarization has a very narrow peak that appears at the frequency of the optical injection.

Some other qualitative features are similar to those found for smaller values of the bias current. Anticorrelation between the power of both linear polarizations appear (see the time traces shown in Figs. 5(a), (c), (e)). Also  $\sigma_T$  increases as  $P_{inj}$ . This can be seen in the values of  $\sigma_T$  and  $C(0)$  corresponding to Fig. 5 that are included in Table 2.

$\Delta\nu/\text{GHz}$	$P_{inj}/\mu\text{W}$	$\langle T \rangle/\text{ns}$	$\sigma_T/\text{ps}$	$C(0)$	$C(\tau_m)$	$\tau_m/\text{ns}$
5	96.1	0.19	7	0.75	0.87	-0.0125
	127.6	0.187	6	0.65	0.65	0
	197.3	0.168	6	0.24	0.24	0
	287.8	0.155	6	-0.013	-0.05	0.0375
-1.5	58.5	0.326	7	-0.37	-0.94	0.0625
	67.6	0.404	10	-0.47	-0.93	0.0625
	84.0	0.38	200	-0.67	-0.77	0.075

Table 2: Averaged interpulse time ( $\langle T \rangle$ ), standard deviation ( $\sigma_T$ ), and correlation coefficient ( $C(0)$ ), first minimum of the cross-correlation function ( $C(\tau_m)$ ) and time at which it appears ( $\tau_m$ ). The applied bias current is 8 mA.

#### IV. SUMMARY AND CONCLUSIONS.

In this work we have made an experimental study of the polarization-resolved nonlinear dynamics of a 1550 nm VCSEL subject to orthogonal optical injection. Our attention has been focused on describing the high-resolution (10 MHz) optical spectra corresponding to both linear polarizations. We have related our spectra with the results previously described in [34] that concern polarization-resolved simultaneous time traces and RF spectra. Different injected powers and detunings between the frequency of the injected signal and the free-running frequency of the VCSEL have been considered. For periodic dynamics, both linear polarizations show spectra with equally spaced peaks, with a separation that corresponds to the frequency detuning. As the injected power increases much more peaks are observed with larger (smaller) separation between them when the frequency detuning is positive (negative) due to the frequency pushing (pulling) effect. For negative values of the frequency detuning, increasing the injected power leads to irregular dynamics that is characterized by optical spectra for both linear polarizations with broad pedestals and much less defined peaks specially for the parallel polarization.

#### ACKNOWLEDGEMENTS

The authors acknowledge support from the Ministerio de Ciencia e Innovación under project TEC2009-14581-C02-02.

## REFERENCES

- [1] J. Ohtsubo, "Semiconductor lasers. Stability, instability and chaos". Springer series in optical sciences. Berlin 2007.
- [2] F. Koyama, "Recent advances of VCSEL Photonics," *J. Lightwave Technol.* vol. 24, no. 12, pp. 4502-4513, Dec. 2006.
- [3] C. J. Chang-Hasnain, J. P. Harbison, G. Hasnain, A. C. Von Lehmen, L. T. Florez, and N. G. Stoffel, "Dynamic, polarization and transverse mode characteristics of vertical-cavity surface-emitting lasers", *IEEE J. Quantum Electron.*, vol. 27, no. 6, pp. 1402-1409, Jun. 1991.
- [4] K. D. Choquette, R. P. Schneider, K. L. Lear, and R. E. Leibenguth, "Gain-dependent polarization properties of vertical-cavity lasers", *IEEE J. Select. Topics Quantum Electron.*, vol. 1, no. 2, pp. 661-666, Mar./Apr 1995.
- [5] R. Gordon, A. P. Heberle, J. R. A. Cleaver, "Transverse mode locking in microcavity lasers", *Appl. Phys. Lett.*, vol. 81, no. 24, pp. 4523-4525, Dec. 2002.
- [6] A. Valle, L. Pesquera, "Turn-off transients in current-modulated multitransverse-mode vertical-cavity surface-emitting lasers", *Appl. Phys. Lett.*, vol. 79, no. 24, pp. 3914-3916, Dec. 2001.
- [7] T. Kim, S. B. Kim, "Suppressing the turn-off induced pulsations in VCSELs using an elevated oxide-layer structure", *Opt. Exp.*, vol. 18, no.2, pp. 1271-1277, Jan. 2010.
- [8] M. J. Adams, A. Hurtado, D. Labukhin, and I. D. Henning, "Nonlinear semiconductor lasers and amplifiers for all-optical information processing", *Chaos*, vol. 20, art. 037102, 2010.
- [9] C. H. Chang, L. Chrostowski, C. J. Chang-Hasnain, "Injection locking of VCSELs," *IEEE J. Select. Topics Quantum Electron.*, vol. 9, no. 5, pp.1386-1393, Sep./Oct 2003.
- [10] D. Parekh, X. Zhao, W. Hofmann, M. C. Amann, L. A. Zenteno and C. J. Chang-Hasnain, "Greatly enhanced modulation response of injection-locked multimode VCSELs," *Opt. Exp.*, vol. 16, no. 26, pp. 21582-21586, Dec. 2008.
- [11] D. Parekh, B. Zhang, X. Zhao, Y. Yue, W. Hofmann, M.C. Amann, A. Willner, and C. J. Chang-Hasnain, "Long distance single-mode fiber transmission of multimode VCSELs by injection locking", *Opt. Exp.*, vol. 18, no.20, pp. 20552-20557, 2010.
- [12] H. Li, T. Lucas, J. G. McInerney, M. Wright, and R. A. Morgan, "Injection locking dynamics of vertical cavity semiconductor lasers under conventional and phase conjugate injection. " *IEEE J. Quantum Electronics*, vol. 32, no. 3, pp. 227-235, Feb. 1996.
- [13] Y. Hong, P. S. Spencer, S. Bandyopadhyay, P. Rees, and K. A. Shore, "Polarization resolved chaos and instabilities in a VCSEL subject to optical injection", *Opt. Comm.*, vol. 216, pp. 185-187, 2003.
- [14] Z. G. Pan, S. Jiang, M. Dagenais, R. A. Morgan, K. Kojima, M. T. Asom, and R. E. Leibenguth, "Optical injection induced polarization bistability in vertical-cavity surface-emitting lasers," *Appl. Phys. Lett.*, vol. 63, no. 22, pp. 2999-3001, Nov.1993.
- [15] D. L. Boiko, G. M. Stéphan, and P. Besnard, "Fast polarization switching with memory effect in a vertical cavity surface emitting laser subject to modulated optical injection," *J. Appl. Phys.* 86, pp. 4096-4099, Oct. 1999.
- [16] Y. Hong, K.A. Shore, A. Larsson, M. Ghisoni, and J. Halonen, "Pure frequency-polarisation bistability in vertical-cavity surface-emitting lasers subject to optical injection", *Electron. Lett.* 36, no. 24, pp. 2019-2020, 2000.
- [17] Y. Hong, P.S. Spencer, P. Rees and K.A. Shore, "Optical injection dynamics of two-mode vertical cavity surface-emitting semiconductor lasers", *IEEE J. Quantum Electronics*, vol. 38, no. 3, pp. 274-278, Mar. 2002.
- [18] J. Buesa, I. Gatara, K. Panajotov, H. Thienpont, and M. Sciamanna, "Mapping of the dynamics induced by orthogonal optical injection in vertical-cavity surface-emitting lasers", *IEEE J. Quantum Electron.*, vol. 42, no. 2, pp. 198-207, Feb. 2006.
- [19] I. Gatara, J. Buesa, H. Thienpont, K. Panajotov, M. Sciamanna, "Polarization switching bistability and dynamics in vertical-cavity surface-emitting lasers under orthogonal optical injection", *Optical and Quantum Electronics*. 38, pp. 429-443, 2006.
- [20] I. Gatara, K. Panajotov, M. Sciamanna, "Frequency-induced polarization bistability in vertical-cavity surface-emitting lasers with orthogonal optical injection", *Phys Rev. A*. 75, 023804, 2007.
- [21] M. Sciamanna and K. Panajotov, "Route to polarization switching induced by optical-injection in vertical-cavity surface-emitting lasers", *Phys. Rev. A*, vol. 73, no. 2, 023811, Feb. 2006.
- [22] I. Gatara, M. Sciamanna, M. Nizette, and K. Panajotov, "Bifurcation to polarization switching and locking in vertical-cavity surface-emitting lasers with optical injection", *Phys. Rev. A*, vol. 76, no. 031803(R), 2007.

- [23] K. Panajotov, I. Gatare, A. Valle, H. Thienpont and M. Sciamanna, "Polarization- and Transverse-Mode Dynamics in Optically Injected and Gain-Switched Vertical-Cavity Surface-Emitting Lasers", *IEEE J. Quantum Electron.* vol.45, no.11, pp.1473-1481, Nov. 2009.
- [24] I. Gatare, M. Sciamanna, M. Nizette, H. Thienpont and K. Panajotov, "Mapping of two-polarization-mode dynamics in vertical-cavity surface-emitting lasers with optical injection," *Phys. Rev. E.*, vol. 80, no. 026218, Aug. 2009.
- [25] M. Nizette, M. Sciamanna, I. Gatare, H. Thienpont, and K. Panajotov, "Dynamics of vertical-cavity surface-emitting lasers with optical injection: a two-mode model approach", *J. Opt. Soc. Am. B*, vol. 26, no. 8, pp. 1603-1613, Aug. 2009.
- [26] A. Valle, M. Gomez-Molina, and L. Pesquera, "Polarization bistability in 1550 nm wavelength single-mode vertical-cavity surface-emitting lasers subject to orthogonal optical injection," *IEEE J. Sel. Top in Quantum Electron.*, vol. 14, no. 3, pp. 895-902, May/Jun.2008.
- [27] A. Hurtado, I. D. Henning, and M. J. Adams, "Two-wavelength switching with a 1550 nm VCSEL under single orthogonal optical injection," *IEEE J. Sel. Top. in Quantum Electron*, vol. 14, no. 3, pp. 911-917, May/Jun.2008.
- [28] K. H. Jeong, K. H. Kim, S. H. Lee, M. H. Lee, B. S. Yoo and K. A. Shore, "Optical injection-induced polarization switching dynamics in 1.5  $\mu\text{m}$  wavelength single-mode vertical-cavity surface-emitting lasers," *IEEE Photon. Technol. Lett.*, vol. 20, no. 9-12, pp. 779-781, May. 2008.
- [29] A. Quirce, A. Valle, and L. Pesquera, "Very wide hysteresis cycles in 1550 nm-VCSELs subject to orthogonal optical injection", *IEEE Phot. Tech. Lett.* 21, no. 17, pp. 1193-1195, 2009.
- [30] A. Hurtado, A. Quirce, A. Valle, L. Pesquera, and M. J. Adams, "Power and wavelength polarization bistability with very wide hysteresis cycles in a 1550nm-VCSEL subject to orthogonal optical injection", *Opt. Exp.* 17, no. 26, pp. 23637-23642, 2009.
- [31] A. Hurtado, A. Quirce, A. Valle, L. Pesquera, and M. J. Adams, "Nonlinear dynamics induced by parallel and orthogonal optical injection in 1550 nm vertical-cavity surface-emitting lasers (VCSELs)", *Opt. Exp.*, vol. 18, no. 9, pp. 9423-9428, 2010.
- [32] P. Perez, A. Quirce, L. Pesquera, and A. Valle, "Polarization resolved nonlinear dynamics induced by orthogonal optical injection in long-wavelength VCSELs", *IEEE J. Sel. Top. Quantum Electron.* vol. 17, pp.1228-1235, Nov. 2011
- [33] R. Al-Seyab, K. Schires, N. A. Khan, A. Hurtado, I. D. Henning, and M. J. Adams, "Dynamics of polarized optical injection in 1550 nm VCSELs: theory and experiments", *IEEE J. Sel. Top. Quantum Electron.* vol. 17, pp.1242-1249, Nov. 2011
- [34] A. Quirce, P. Perez, A. Valle, and L. Pesquera, "Correlation properties and time-resolved dynamics of linear polarizations emitted by single-mode vertical-cavity surface-emitting lasers subject to orthogonal optical injection", *J. Opt. Soc. Am. B*, vol. 28, no. 11, pp. 2765-2776, Nov. 2011.